An Air Gap Model for Magnetostatic Volume Integral Formulation

Mayra Hernandez Alayeto, Gerard Meunier, Loic Rondot, Olivier Chadebec, Matthieu Favre, Jean-Michel Guichon

An Air Gap Model for Magnetostatic Volume Integral Formulation

Mayra Hernandez Alayeto[1, 2], Gérard Meunier[1], Loic Rondot[2], Olivier Chadebec[1], Matthieu Favre[2] and Jean-Michel Guichon[1]

[1]Univ. Grenoble Alpes, CNRS, Grenoble INP, G2ELab, Grenoble, France
[2]Schneider Electric, Global Technology Eybens, France

The presence of air gaps in magnetic modeling problems is well known. When the air gap is thin, its numerical treatment is complex because the integrals arising on the model lead to inaccuracy. This paper presents an air gap model for thin air gaps using the magnetostatic volume integral method for linear and non linear problems. The thin air gap is considered as a face region with a numerical treatment to improve the accuracy. An application to an academic case and a current transformer is reported to validate the model.

***Index Terms*—Volume integral method, air gap, magnetostatics, facet element.**

I. Introduction

VOLUME integral method (VIM) is a powerful approach to solve magnetic problems. Contrary to the finite element method (FEM), only the active regions have to be discretised, thus avoiding to mesh the air. The VIM started in 1970s with the magnetic moment method, based on uniform magnetization on each element [1] but it wasn't until the last decade that it became more popular as a result of three main improvements: advanced integral formulations such as [2] [3] (H-conforming formulations) or [4] (B-conforming formulation), matrix compression algorithms such as the fast multipole method (FMM) [5] or hybrid cross approximation (HCA) [6] and the increase of computers RAM memory. A VIM based on facet elements for linear and non linear problems [4] is considered in this paper.

A frequent feature of magnetic problems is the presence of air gaps, that can be very thin, arising for example when two parts are welded. Modeling air gaps presents difficulties, there are two options to do it. The first is to not mesh the air gap, then the proximity of the two air gap faces leads to inaccurate integral computations of Green's kernel. The second option is to mesh the air gap as a volume element, this case is more accurate than not meshing the air gap but it also leads to difficult integral calculations on the mesh elements of the air gap because the two air gap faces are very close.

A third alternative is presented in this paper: a VIM model of thin air gaps considered as a face region. It avoids the numerical treatment difficulty that arises when the air gap is not meshed. It also allows to avoid a thin mesh of the air gap volume region that is computationally expensive, meshing only the face of the air gap and keeping the precision of computations. This strategy has already been done on a FEM approach for a B-conforming formulation [7] and a H-conforming formulation [8], [9]. Nevertheless, for the VIM case, special attention has to be given to the integral equations that model the air. The face air gap development is applied to an academic case and an industrial example and it is compared with a converged volume air gap model to show its accuracy.

This paper is organised as follows: section II explains the volume integral formulation using B-facet elements, section III describes the face air gap model developed for the previous formulation, section IV presents two applications of the face air gap model and finally a conclusion in section V completes the paper.

Manuscript received XXX; revised XXX. Corresponding author: M. Hernandez Alayeto (email: mayra.hernandezalayeto@se.com).

II. Volume Integral Formulation

We consider Maxwell's equations under magnetostatics assumptions in a domain composed of a ferromagnetic region Ω and coils. The volume magnetostatic integral equation in terms of induction $\mathbf{B}$ [4] is:

$$\nu\mathbf{B} + \frac{1}{4\pi}\boldsymbol{\nabla}\left(\int_{\Omega}((\nu_0 - \nu)\mathbf{B}) \cdot \boldsymbol{\nabla}\left(\frac{1}{\mathrm{r}}\right)\mathrm{d}\Omega\right) = \mathbf{H_0} \tag{1}$$

where ν is the reluctivity of the ferromagnetic region that depends on $\mathbf{B}$, ν_0 is the vacuum reluctivity, $\boldsymbol{\nabla}$ is the differential operator, r is the distance between the integration point and the observation point and $\mathbf{H_0}$ is the source field created by source currents.

Interpolating $\mathbf{B}$ with facet elements (Whitney 2-form [10]) and applying a Galerkin projection with facet functions as in [4], the resulting discretized integral system reads

$$(\mathbf{R} + \mathbf{L})\{\Phi\} = \{\Delta\varphi\} + \{\mathrm{S}\} \tag{2}$$

where Φ is the magnetic flux across each facet of the mesh, $\Delta\varphi$ is the difference of magnetic potential of two mesh elements, S is a term coming from the external sources, $\mathbf{R}$ is the finite element matrix

$$\mathrm{R_{ij}} = \int_{\Omega} \mathbf{w_i} \cdot \nu\mathbf{w_j}\mathrm{d}\Omega \tag{3}$$

where $\mathbf{w_i}$ is the facet shape function of element i and $\mathbf{L}$ is the integral full matrix

$$\mathrm{L_{ij}} = \frac{1}{4\pi}\int_{\Gamma_{\mathrm{ext_i}}} \frac{1}{\mathrm{s_i}} \int_{\Gamma_{\mathrm{j}}} \frac{1}{\mathrm{s_j}}\delta\nu_{\mathrm{j}}\frac{1}{\mathrm{r}}\mathrm{d}\Gamma_{\mathrm{j}}\mathrm{d}\Gamma_{\mathrm{ext_i}} \tag{4}$$

where s_i is the surface of the facet element i, $\delta\nu$ is the reluctivity jump between two adjacent elements that have a shared facet, Γ is the ensemble of facets of the problem and Γ_{ext} refers only to the facets that are on the boundary of the ferromagnetic region. Let us notice that for the non linear case the hypothesis of ν being constant at each mesh element is considered, which is already true for tetrahedral mesh elements because in that case **B** is constant at each element. The non linear resolution of the system is carried out with the Newton-Raphson method.

In practice, eq. (2) is a representation of the problem with an equivalent electric circuit approach expressed with a dual mesh as in Fig. 1 [12], where the branches of the dual mesh correspond to the facets of the primal mesh and the nodes of the dual mesh are the elements of the primal mesh. Then **R** matrix can be seen as the internal reluctance matrix for the magnetic material and **L** matrix as the one taking into account flux in air region. To solve the problem, either the Kirchhoff's nodal rule or the Kirchhoff's mesh rule can be used. This procedure ensures the free divergence of **B**.

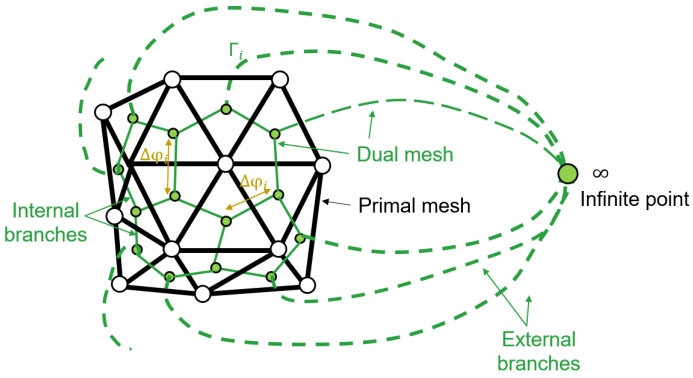

Fig. 1: Primal mesh and dual mesh of a region.

In order to speed the computations, a matrix compression technique needs to be used, such as FMM [5] on matrix **L**. To that aim, we apply an iterative solver with GMRES that can be accelerated with the use of a preconditioner of type LU on the finite element matrix **R**.

III. Face Air Gap Model

Let us consider the following assumptions:

- Thickness of the air gap is small compared to the dimension of the other elements.
- Flux leakage from the external faces of the air gap is null.
- Flux inside the air gap is perpendicular to the air gap. We can assume this because the permeability of the material is much higher than the permeability of the vacuum and the air gap is thin.

Due to these assumptions, the air gap can be considered as a face region instead of a volume region (Fig. 2). The equivalent magnetic circuit can be built adding the air gap contribution to matrices **R** and **L** (eqs. (3) and (4)). For the finite element matrix **R**, an additional reluctance on the mesh branches that cross the air gap is considered, given by $\frac{\mu_0 e}{s}$, where e is the

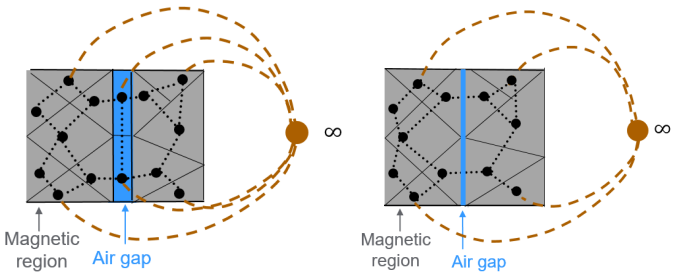

Fig. 2: Equivalent magnetic circuit of a device for an air gap as volume region (left) and as face region (right).

thickness of the air gap, s is the surface of the facet element and μ_0 is the vacuum permeability. This can be seen as the relutance of a parallelepiped of surface s and depth e. For matrix **L**, since the air gap is characterized by having two regions that are near, the evaluation on two parallel faces Γ_1 and Γ_2 that are in front of each other and separated by a distance equal to the thickness of the air gap (Fig. 3) is given by:

$$\frac{1}{4\pi}\int_{\Gamma_{\text{ext}_i}}\frac{1}{s_i}\int_{\Gamma_{1_j}}\frac{1}{s_j}(\nu_1-\nu_0)\frac{1}{r_1}d\Gamma_{1_j}d\Gamma_{\text{ext}_i}- \frac{1}{4\pi}\int_{\Gamma_{\text{ext}_i}}\frac{1}{s_i}\int_{\Gamma_{2_j}}\frac{1}{s_j}(\nu_2-\nu_0)\frac{1}{r_2}d\Gamma_{2_j}d\Gamma_{\text{ext}_i} \quad (5)$$

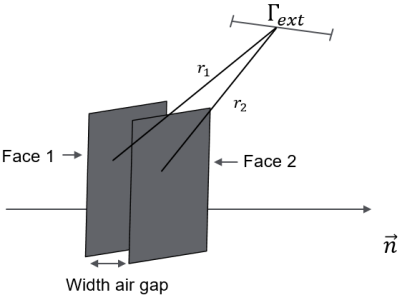

Fig. 3: Air gap representation.

where Γ_{1_j} are the facet elements j that are on face Γ_1 and minus sign between the two previous terms comes from the orientation of the faces, going from Γ_1 to Γ_2. Now, expressing ν_1 and ν_2 as $\nu_1 = \nu_{\text{avg}} + \frac{\delta\nu}{2}$, $\nu_2 = \nu_{\text{avg}} - \frac{\delta\nu}{2}$ where $\nu_{avg} = \frac{\nu_1+\nu_2}{2}$ and $\delta\nu = \frac{\nu_1-\nu_2}{2}$, the previous expression becomes:

$$\frac{1}{4\pi}\int_{\Gamma_{\text{ext}_i}}\frac{1}{s_i}\frac{\delta\nu}{2}\frac{1}{s_j}\Big[\int_{\Gamma_{1_j}}\frac{1}{r_1}d\Gamma_{1_j}-\int_{\Gamma_{2_j}}\frac{1}{r_2}d\Gamma_{2_j}\Big]d\Gamma_{\text{ext}_i}- \frac{1}{4\pi}\int_{\Gamma_{\text{ext}_i}}\frac{1}{s_i}(\nu_{\text{avg}}-\nu_0)\Big[\int_{\Gamma_{1_j}}\frac{1}{r_1}d\Gamma_{1_j}-\int_{\Gamma_{2_j}}\frac{1}{r_2}d\Gamma_{2_j}\Big]d\Gamma_{\text{ext}_i}. \quad (6)$$

The latter equation shows that when the air gap is thin r_1 and r_2 are almost the same value and then the difference between the two large terms involving r_1 and r_2 can lead to inaccuracy. This happens when the air gap is meshed as a volume element and when it is not meshed at all. Nevertheless, when it is meshed as a volume element the inaccuracy is only given on matrix **L** whereas if there is no air gap mesh, inaccuracy is given on both matrices **R** and **L**.

For the face air gap model, the first term can be approximated as:

$$\frac{1}{4\pi}\int_{\Gamma_{\mathrm{ext_i}}}\frac{1}{\mathrm{s_i}}\int_{\Gamma_\mathrm{j}}\frac{1}{\mathrm{s_j}}\frac{\delta\nu}{\mathrm{r}}\mathrm{d}\Gamma_\mathrm{j}\mathrm{d}\Gamma_{\mathrm{ext_i}} \tag{7}$$

using a first order Taylor expansion $\frac{1}{\mathrm{r_1}}+\frac{1}{\mathrm{r_2}}=\frac{2}{\mathrm{r}}+\varepsilon(\mathrm{O}^2)\approx\frac{2}{\mathrm{r}}$, where $\varepsilon(\mathrm{O}^2)$ is a term of order two.

The second term is approximated as:

$$\frac{1}{4\pi}\int_{\Gamma_{\mathrm{ext_i}}}\frac{1}{\mathrm{s_i}}\int_{\Gamma_\mathrm{j}}(\nu_{\mathrm{avg}}-\nu_0)\frac{\mathrm{e}}{\mathrm{s_j}}\boldsymbol{\nabla}(\frac{1}{\mathrm{r}})\cdot\mathbf{n}\mathrm{d}\Gamma_\mathrm{j}\mathrm{d}\Gamma_{\mathrm{ext_i}} \tag{8}$$

given that $\boldsymbol{\nabla}(\frac{1}{\mathrm{r}})\cdot\mathbf{n}=\frac{\mathrm{d}}{\mathrm{d}\mathbf{n}}(\frac{1}{\mathrm{r}})\approx\lim_{\mathrm{e}\to0}\frac{\frac{1}{\mathrm{r_1}}-\frac{1}{\mathrm{r_2}}}{\mathrm{e}}$, therefore $\frac{1}{\mathrm{r_1}}-\frac{1}{\mathrm{r_2}}\approx\mathrm{e}\boldsymbol{\nabla}(\frac{1}{\mathrm{r}})\cdot\mathbf{n}$.

Assembling the previous information, matrix $\mathbf{L}$ can be written as:

$$\begin{aligned}\mathrm{L_{ij}}=&\frac{1}{4\pi}\int_{\Gamma_{\mathrm{ext_i}}}\frac{1}{\mathrm{s_i}}\int_{\Gamma_\mathrm{j}}\frac{1}{\mathrm{s_j}}\frac{\delta\nu}{\mathrm{r}}\mathrm{d}\Gamma_\mathrm{j}\mathrm{d}\Gamma_{\mathrm{ext_i}}+\\&\frac{1}{4\pi}\int_{\Gamma_{\mathrm{ext_i}}}\frac{1}{\mathrm{s_i}}\int_{\Gamma_\mathrm{j}}(\nu_{\mathrm{avg}}-\nu_0)\frac{\mathrm{e}}{\mathrm{s_j}}\boldsymbol{\nabla}(\frac{1}{\mathrm{r}})\cdot\mathbf{n}\mathrm{d}\Gamma_\mathrm{j}\mathrm{d}\Gamma_{\mathrm{ext_i}}.\end{aligned} \tag{9}$$

We observe that the first term of $\mathbf{L}$ corresponds to (4), which doesn't consider the air gap, being the second term the additional contribution given by the air gap.

When the thickness of the air gap is small the correction of $\mathbf{R}$ matrix is enough to model the air gap behaviour. Otherwise, the additional correction to $\mathbf{L}$ matrix must be considered.

IV. Applications

A. Academic case

The proposed air gap model is applied to a magnetic part (linear isotropic material with permeability $\mu_r = 1,000$) with an air gap and a coil of 1,000 turns and 1A of imposed current as Fig. 4 shows.

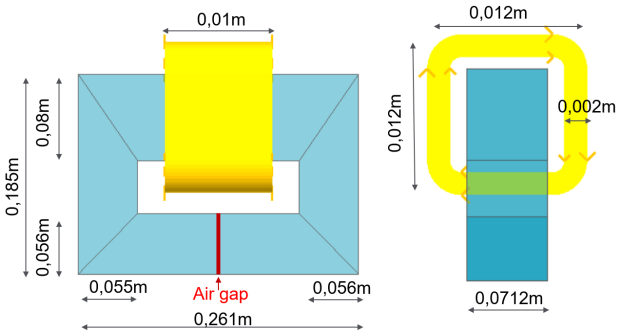

Fig. 4: Academic case geometry.

In order to validate the face region air gap method, the calculation of the magnetic flux through the coil following [11] is compared with the values obtained when the air gap is considered as a volume region. We create a mesh with enough number of elements to have a converged solution on the air gap volume model so that it will be the reference. This mesh has 42,334 tetrahedral elements in the magnetic region and around 1,900 elements in the volume air gap (varying depending on the air gap size). We will mesh the face air gap region with 126 elements. Results for three different air gap thicknesses of 20μm, 30μm and 50μm are given in Fig. 5 and 6.

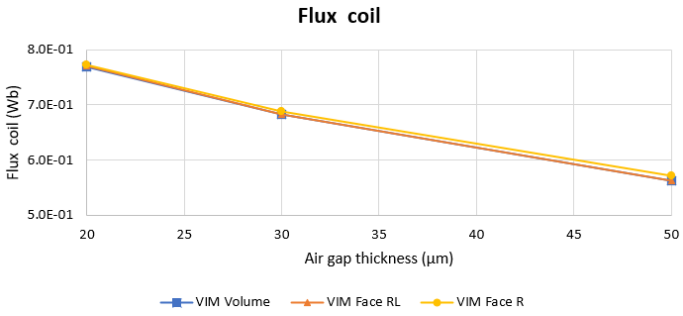

Fig. 5: Flux through coil.

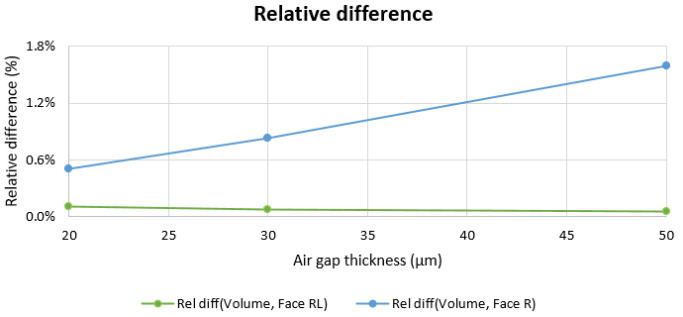

Fig. 6: Relative difference for different air gap thickness.

In Fig. 5 and 6 *VIM volume* refers to the model considering the air gap as a volume region, *VIM face RL* the model when the air gap is a face region with the contribution of $\mathbf{R}$ matrix and $\mathbf{L}$ matrix and *VIM face R* for a face air gap model only with the contribution of $\mathbf{R}$. The relative difference (A,B) at each point is the value obtained in A case minus the value obtained in B case over the value obtained in B case.

Figure 6 shows that the relative difference between the air gap as a volume region and the air gap as a face region using the contribution of matrices $\mathbf{R}$ and $\mathbf{L}$ is very low, inferior to 0.2% and it is stable for the three air gaps tested. The difference between the air gap as a volume region and the air gap as a face region using only the contribution of matrix $\mathbf{R}$ remains inferior to 2% for the three air gaps tested, but it increases as the air gap thickness enlarges.

The conclusion for this application is that adding the contribution to both matrices $\mathbf{R}$ and $\mathbf{L}$ provides more accurate and more stable results.

B. Industrial case

The second validation case is a current transformer composed of two coils and a ferromagnetic region with a non linear material that follows an isotropic analytic saturation of arc tangent type with two coefficients, μ_r =100 and saturation magnetization = 1.2T as Fig. 7 shows.

The air gap is produced when welding the magnetic part, which is opened in order to introduce the coil inside the device, thus producing and air gap on a face region of the current transformer.

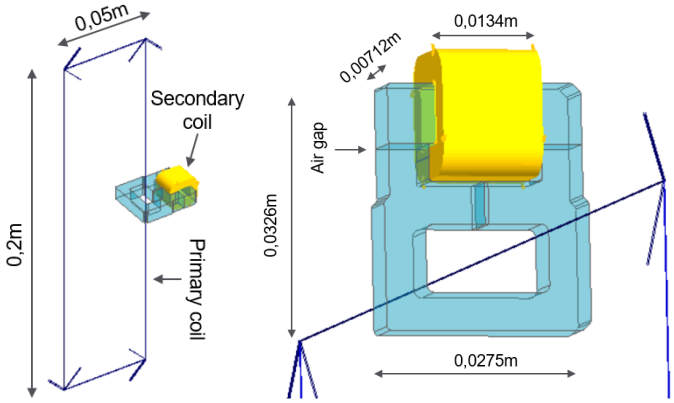

Fig. 7: Geometry of magnetic region (light blue), primary coil (dark blue) and secondary coil (yellow).

The primary coil has 1 turn and an imposed current of 10A, the secondary coil has 980 turns and no current imposed. In order to validate the face region air gap method, we follow the same method as the academic case, comparing the flux through the secondary coil for a model of a volume air gap with a converged mesh (reference) and the face air gap model. The converged mesh has 39,165 tetrahedral elements in the magnetic region and around 500 elements in the volume air gap. The face air gap region has 160 elements. Results for three different air gap thicknesses of 20μm, 30μm and 50μm are given in Fig. 8 and Fig. 9.

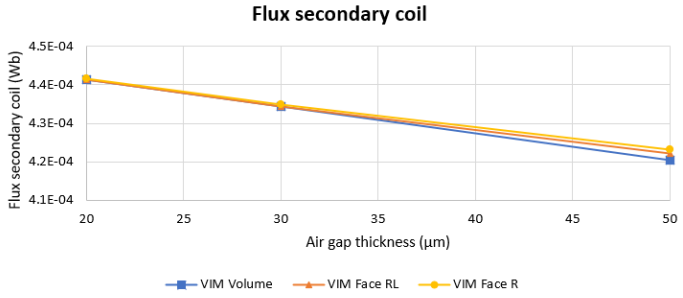

Fig. 8: Flux through secondary coil.

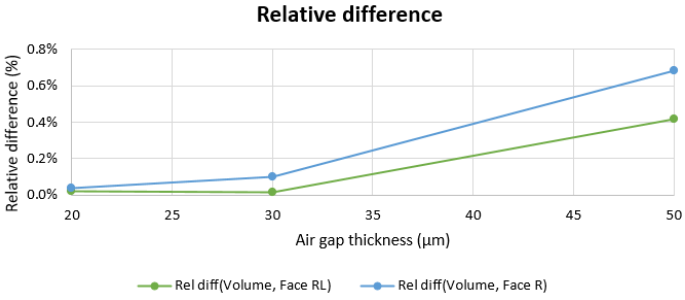

Fig. 9: Relative difference for different air gap thickness.

Figure 9 shows that the face and volume models provide closer results for thin air gaps, increasing the difference when the air gap is thicker . It is also exhibited that the contribution of both matrices **R** and **L** presents lower relative difference to the volume model than considering the contribution of matrix **R** only.

In terms of computation time of the problem, the face air gap model is less time consuming than the volume air gap model, taking around 180 seconds to solve the face air gap model (**R** and **L** contributions) and roughly 330 seconds for the volume one. The time difference might be due to the higher number of mesh elements in the volume air gap region compared to the number of elements of the face air gap region.

This application provides a second validation of the VIM face air gap model.

V. Conclusion

A model of thin air gaps using the VIM is proposed. It considers the air gap as a face region with a given thickness, avoiding the integration difficulties that produces not meshing the air gap or meshing it as a volume region. It is made for a **B**-facet volume integral formulation for linear and non linear magnetostatic problems [4].

It adds new terms on matrices **R** and **L** of the system that defines the problem, showing that for thin air gaps the contribution on matrix **R** can be enough, but for thicker air gaps both contributions are needed.

An application to an academic case and an industrial case are shown for different air gap thicknesses, keeping the accuracy of the model more thoroughly when the air gap is thinner.

References

[1] MJ Newman, CW Trowbridge and LR Turner, “GFUN: An interactive program as an aid to magnet design,” ” in Proc. 4th Int. Conf. Magn. Technol., Upton, NY, USA, 1972, pp. 617–626.

[2] A. Carpentier, O. Chadebec, N. Galopin, G. Meunier and B. Bannwarth, “Resolution of Nonlinear Magnetostatic Problems With a Volume Integral Method Using the Magnetic Scalar Potential,” IEEE Trans. Magn., vol. 49, no. 5, pp. 1685–1688, 2013.

[3] A. Canova and M. Repetto, “Integral solution of nonlinear magnetostatic field problems,” IEEE Trans. Magn., vol. 37, no. 3, pp. 1070–1077, May 2001.

[4] V. Le-Van, G. Meunier, O. Chadebec and J-M Guichon, “A Volume Integral Formulation Based on Facet Elements for Nonlinear Magnetostatic Problems,” IEEE Trans. Magn., vol. 51, no. 7, July 2015.

[5] L. Greengard and V. Rokhlin, “A Fast Algorithm for Particle Simulations,” J. Comput. Phys., vol. 73, no. 2, pp. 325–348, 1987.

[6] S. Börm and L. Grasedyck, “Hybrid cross approximation of integral operators,” Numer. Math., vol. 101, no. 2, pp. 221–249, Jun. 2005.

[7] T. Nakata, N. Takahashi, K. Fujiwara and Y. Shiraki, “3D magnetic field analysis using special elements," IEEE Trans.n Magn., vol. 26, no. 5, pp. 2379-2381, 1990.

[8] C. Guérin, G. Tanneau, G. Meunier, X. Brunotte and J. B. Albertini, “Three dimensional magnetostatic finite elements for gaps and iron shells using magnetic scalar potentials, " IEEE trans. magn., vol. 30, no.5, pp. 2885-2888, 1994.

[9] Ospina, A., Santandrea, L., Le Bihan, Y. and Marchand, C. “Modeling of thin structures in eddy current testing with shell elements," The European Physical Journal-Applied Physics, vol. 52, no. 2, 2010.

[10] A. Bossavit, “Whitney forms: A class of finite elements for threedimensional computations in electromagnetism,” IEE Proc. A Phys. Sci., Meas. Instrum., Manage. Edu.-Rev., vol. 135, no. 8, pp. 493–500, Nov. 1988.

[11] L. Huang, G. Meunier, O. Chadebec, J-M Guichon, Y. Li and Z. He, “General Integral Formulation of Magnetic Flux Computation and its Application to Inductive Power Transfer System,” IEEE Trans. Magn., vol. 53, no. 6, June 2017.

[12] T.-T. Nguyen, G. Meunier, J.-M. Guichon, O. Chadebec, and T.-S. Nguyen, “An integral formulation for the computation of 3-D eddy current using facet elements,” IEEE Trans. Magn., vol. 50, no. 2, pp. 549–552, Feb. 2014.